

Cite this: *Chem. Sci.*, 2018, 9, 2098

New application of phthalocyanine molecules: from photodynamic therapy to photothermal therapy by means of structural regulation rather than formation of aggregates†

Xingshu Li,‡ Xiao-Hui Peng,‡ Bing-De Zheng, Jilin Tang, Yuanyuan Zhao, Bi-Yuan Zheng, Mei-Rong Ke and Jian-Dong Huang ^{*}

Phthalocyanine (Pc) molecules exhibit high extinction coefficients in near-infrared region, rendering them well-suited for phototherapies, but most of their applications are limited to the field of photodynamic therapy (PDT). Herein, for the first time, we illustrate that Pc molecules can be endowed with excellent photothermal properties by means of structural regulation rather than formation of aggregates. Three representative Pc derivatives show efficient activities of photothermal therapy (PTT) against human hepatocellular carcinoma cells. Among them, copper phthalocyanine (PcC1) exhibits a high *in vivo* PTT efficacy against mice bearing S180 tumors. The unique investigation in this article should light up a perspective of Pc's new applications for PTT, which enable to make up the inherent defects of PDT.

Received 1st December 2017

Accepted 4th January 2018

DOI: 10.1039/c7sc05115h

rsc.li/chemical-science

Introduction

Phthalocyanine (Pc), a type of molecular dye, has been widely used as a photosensitizer for photodynamic therapy (PDT) because of their long absorption wavelengths ($\lambda_{\max} > 660$ nm), high extinction coefficients ($\epsilon_{\max} > 10^5$ L mol⁻¹ cm⁻¹), and tunable photophysical and photochemical properties *via* facile chemical modifications.¹ To date, one Pc (Aluminium Pc, Photosens®, Russia) has been approved for clinical use and two Pcs (Silicon Pc, Pc4®, USA and Zinc Pc, Photocyanine®, China) have currently reached clinical testing.² For cancer treatment, PDT has been displaying several advantages over chemotherapy owing to its spatiotemporal selectivity and no initiating resistance.³ However, PDT also shows its inherent drawbacks along with the further clinical studies. One of these drawbacks is that patients have to stay in dark for a long period of time during and after treatment, otherwise the unwished photosensitive reaction induced by sunlight or indoor bright light would be harmful to their eyes, skin, and other healthy tissues.⁴ This really causes inconvenience to patients. Moreover, hypoxic nature of tumor microenvironment limits the effectiveness of PDT due to its oxygen-dependent active mechanism.⁵

Recently, photothermal therapy (PTT) has been developed as a new technique for cancer treatment, by which sufficient optical energy (usually from a relatively high-energy laser source) absorbed by photothermal agents can be converted into thermal energy and generate local hyperthermia, leading to irreversible tumor cell injury.⁶ Since the energy of common sunlight or indoor bright light is too low to induce the photothermal agents to generate harmful heating effect, patients do not need to stay in dark during or after PTT treatment. Moreover, its oxygen-independent nature makes PTT more useful for treating hypoxic tumors.⁷ However, only few studies to date have investigated the application of Pcs for PTT.⁸ In addition, all these investigations were based on the formation of Pc aggregates to induce photothermal effects. As shown in Fig. S1,† vibrational relaxation mechanism is the active process involved in PTT.⁹ Therefore, inhibiting or reducing the other two relaxation pathways of an excited Pc through fluorescence emission and intersystem crossing should elevate its photothermal effect. Although the Pc aggregations provide a potential strategy to increase Pc's photothermal effect as a consequence of the reduction of fluorescence emission and intersystem crossing, this strategy unfortunately suffers from the following problems: (1) the formation of aggregates not only requires lots of Pc molecules, but also induces the broadening and decrease in absorption spectrum, leading to a low efficiency of photothermal conversion; (2) the potential transformation between aggregates and monomers makes this PTT application unstable and less repeatable.

Herein, we present that Pc monomers can also be endowed with an excellent photothermal effect through appropriate

College of Chemistry, State Key Laboratory of Photocatalysis on Energy and Environment, Fujian Provincial Key Laboratory of Cancer Metastasis Chemoprevention and Chemotherapy, Fuzhou University, Fuzhou 350108, China. E-mail: jdhuang@fzu.edu.cn

† Electronic supplementary information (ESI) available: Experiment materials and methods, characterization data, additional data. See DOI: 10.1039/c7sc05115h

‡ These authors contributed equally to this work.



structural regulations. Our strategies can be termed as a substituent photoinduced electron transfer (PET)-induced route and a paramagnetic metal-induced pathway. Based on these two strategies, we obtained three representative Pc compounds that display excellent photothermal effects, which are much higher than those of the widely used indocyanine green (ICG) and methylene blue (MB). *In vitro* and *in vivo* studies indicate that these unique Pc compounds are highly promising for PTT application, which will certainly rejuvenate their wide application in cancer phototherapy.

Results and discussion

1. PET-induced route by tuning peripheral substituents

Numerous studies have shown that PET effect induced by a special substituent (*e.g.*, amino group) on the Pc structure can efficiently quench Pc's fluorescence emission and reactive oxygen species (ROS) generation.¹⁰ Thus, we first compared the photothermal effect of two Pc compounds peripherally substituted with amino groups (PcA1 and PcA2). Their chemical structures are displayed in Fig. 1a. Despite their similar structures, PcA1 and PcA2 show very different fluorescence emission and singlet oxygen (¹O₂) generation (Table S1[†], Fig. 1b and c),

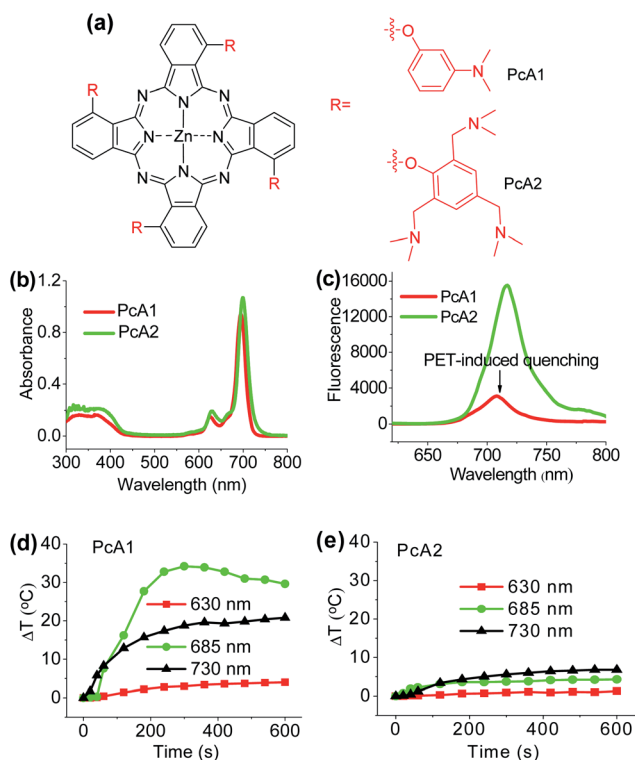


Fig. 1 (a) Chemical structures of PcA1 and PcA2. Only the major C_{4h} isomers are shown for tetra-substituted Pcs, which likely present the other isomers. (b) Electronic absorption and (c) fluorescence spectra (excited at 610 nm) of PcA1 and PcA2 (both at 4 μM) in DMF. Temperature variation profiles of (d) PcA1 and (e) PcA2 (both at 10 μM) in water with 0.1% CEL after being exposed to different laser irradiations (630 nm, 685 nm, and 730 nm, power densities are controlled at 1.0 W cm⁻²).

which are possibly quenched by the PET effect in PcA1 induced by its aniline groups. In PcA2, the spacers (methylene) between amino and phenoxy groups reduce the electronic coupling of amino groups and Pc macrocycle, leading to a much weaker PET effect. In water with 0.1% Cremophor EL (CEL is a common surfactant that is often utilized for improving the water solubility and disaggregation of photosensitizers),^{16,6c,11} upon irradiation at 685 or 730 nm laser, PcA1 permits a strong photothermal conversion, while PcA2 almost has negligible photothermal effect at all the three irradiated wavelengths (Fig. 1d, e and S2[†]). We also find that the photothermal effect of PcA1 is dependent on the laser wavelength. Laser with a wavelength around the maximal absorption wavelength of non-aggregated PcA1 absorption spectrum (Fig. 1b), such as 685 nm, can induce a higher temperature elevation.

To evaluate phototherapeutic effect mediated by PcA1 and PcA2 *in vitro*, human hepatocarcinoma (HepG2) cells were incubated with 10 μM of these Pc compounds and exposed to a laser irradiation (730 nm, 1.0 W cm⁻²) for 10 min. Given the same absorbance of PcA1 and PcA2 around 730 nm in water with 0.1% CEL (Fig. S3[†]), we thus compared their phototherapeutic effects using 730 nm-laser. Cell viability measurements show about 90% HepG2 cell death for both PcA1 and PcA2 when compared with the controls (Fig. 2a). In contrast, negligible cytotoxicity was observed for both PcA1 and PcA2 under dark conditions or laser irradiation alone. To explain their therapeutic mechanisms, we assessed the alterations in intracellular temperature and ROS during treatment. Following laser irradiation, the temperature inside PcA1-treated cells increased by 15 °C, reaching a value of 45 °C (Fig. 2b), which is slightly higher than the required temperature of hyperthermia (42 °C).¹² However, a temperature increase in PcA2-treated cells

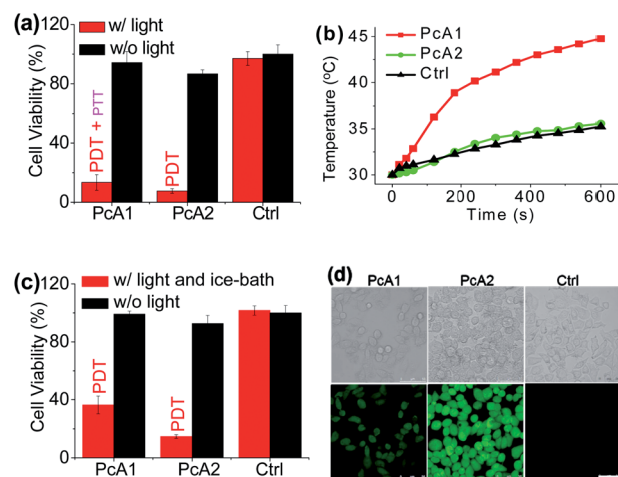


Fig. 2 (a) Cytotoxic effect of PcA1 and PcA2 (both at 10 μM) on HepG2 cells in the presence and absence of laser irradiation (730 nm, 1.0 W cm⁻², 10 min). w/: with. w/o: without. Ctrl: control. (b) Temperature profiles of HepG2 cells induced by PcA1 and PcA2 under laser irradiation. Non-treated cells with laser were used as the control. (c) Cytotoxic effect of PcA1 and PcA2 on HepG2 cells after controlling the temperature of cells at less than 30 °C using an ice-bath during laser treatment. (d) ROS levels in HepG2 cells induced by PcA1 and PcA2. Scale bars = 50 μm.



is as low as that in the non-treated cells ($\sim 5^\circ\text{C}$). Furthermore, we evaluated their phototherapeutic effect again using an ice-bath to control the cells' temperature lower than 30°C during laser irradiation. This method was also used by other groups to further explain the cell killing effect of PTT agent caused by temperature increase.¹³ As shown in Fig. 2c, the cell inhibition effect induced by PcA1 reduces to $64.6 \pm 6.0\%$, while the PcA2 group shows a very similar result with the abovementioned group with no ice-bath treatment. These results confirm that PcA1 possesses some PTT effect, but not PcA2. In addition to the photothermal effect, it is further investigated that the PDT mechanism is also activated during the PcA1 treatment. As indicated in Fig. 2d, the intracellular ROS level increases following irradiation of PcA1-treated cells in spite of the higher ROS level induced by PcA2.

Different from the only PDT effect of PcA2, PcA1 shows combined PTT ($\sim 30\%$) and PDT ($\sim 70\%$) effects. To identify the cause of PTT effect, we further used different ratios of CEL to control Pcs' aggregation in water and test their photothermal conversions. Fig. S4† indicates that PcA1 in low aggregated formation still has a strong heating effect, which is similar to that of PcA1 in high aggregated formation, indicating that the aggregation of PcA1 does not help in increasing the heating effect. Moreover, PcA2 (Fig. S5†) and PcA3 (another Pc compound without PET effect, Fig. S6†) show negligible heating effect either in aggregated form or in monomer form. Therefore, the PET effect-induced low fluorescence emission and ROS generation should be the main contributors for PcA1's PTT effect.

The above results demonstrate that the Pc candidates exhibit good PTT effect, which can be achieved by regulating their peripheral substituents. Since there are countless chemical groups that can be substituted onto the peripheral positions of Pc structure, more promising Pcs with higher heating effect are expected to be broadly developed for PTT.

2. PET-induced route by altering axial ligands

Secondly, following the direction of PET effect, we found that the PTT and PDT efficacy of Pc compounds also can be controlled by tuning their axial substituents. Because of the PET effect, silicon Pc axially substituted with piperazine groups (PcB1, Fig. 3a) has low fluorescence quantum yield (Φ_F) and $^1\text{O}_2$ quantum yield (Φ_Δ) (Table S1 and Fig. S7†), indicating that PcB1 may possess PTT effect.

From Fig. S8a,† the temperature of PcB1 aqueous solution (containing 0.1% CEL) increased rapidly with irradiation time and reached a temperature variation (ΔT) of 28°C . As a control, PcB2, that has no PET effect because of the quaternization of piperazine groups (Fig. 3a), shows weak photothermal conversion (Fig. S8b†). In addition, Fig. S9a† shows that the higher ratio of CEL makes PcB1 to be aggregated in water to a lower extent, accompanied with an increase in absorption. Interestingly, the higher CEL ratio also makes its photothermal conversion more efficient (Fig. S9b†).

To evaluate the *in vitro* phototoxic effects of PcB1, we still used HepG2 cells. As shown in Fig. 3b, the cell viability decreases to $32.0 \pm 2.7\%$ at $5\ \mu\text{M}$ of PcB1 under laser

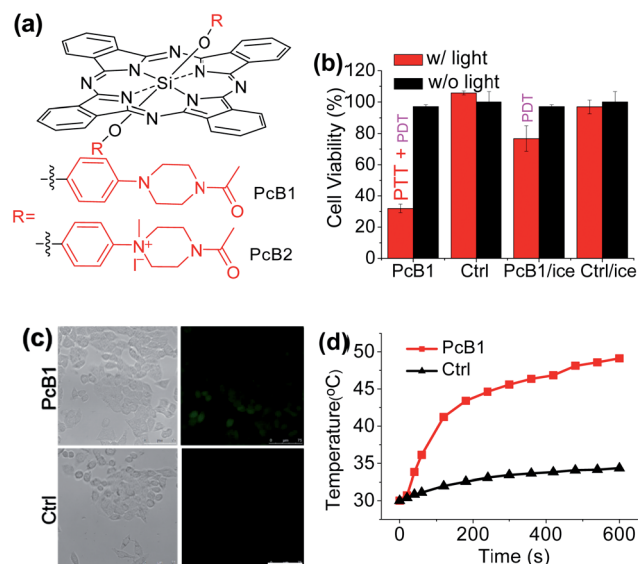


Fig. 3 (a) Chemical structures of PcB1 and PcB2. (b) Cytotoxic effect of PcB1 on HepG2 cells with and without laser irradiation. PcB1/ice and Ctrl/ice mean controlling the temperature of cells at below 30°C via an ice-bath during laser treatment. (c) ROS levels in HepG2 cells induced by PcB1 under laser irradiation. Scale bars = $75\ \mu\text{m}$. (d) Temperature variation profile of HepG2 cells incubated with PcB1 ($5\ \mu\text{M}$) and exposed to the laser irradiation ($730\ \text{nm}$, $1.0\ \text{W cm}^{-2}$). Non-treated cells exposed to the laser were used as the control.

irradiation. However, after using an ice-bath, this cell viability becomes $76.7 \pm 8.1\%$. Furthermore, the ROS generation induced by PcB1 under laser irradiation in HepG2 cells was also evaluated. As shown in Fig. 3c, the fluorescent signal of ROS probe in PcB1-treated cells exhibits a little signal compared with that of control group. Moreover, the cellular temperature of PcB1-treated cells without an ice-bath was much higher than that of the control group (Fig. 3d). Thus, we can summarize that PcB1 displays a combination of PTT and PDT. In addition, the PTT effect ($\sim 70\%$) of PcB1 is higher than its PDT effect ($\sim 30\%$).

3. Paramagnetic metal-induced pathway by changing central metal ions

It has been explored that Pc macrocycle structures are able to chelate a diverse range of metals ions including Zn^{2+} , Si^{4+} , Al^{3+} , Cu^{2+} , Co^{2+} , Ni^{2+} , Fe^{2+} , Fe^{3+} , Mn^{2+} , Cd^{2+} , Ga^{3+} , Pd^{2+} , and Pt^{2+} .¹⁴ The photophysical properties of Pc compounds are drastically influenced by the presence and nature of the central metal ion. Closed shell diamagnetic ions, such as Zn^{2+} , Si^{4+} , and Al^{3+} , afford Pc complexes with both high intersystem crossing effect and long triplet lifetimes.¹⁵ As a result, these complexes (ZnPc , SiPc , and AlPc) usually show strong photochemical and photodynamic activities and unsurprisingly become the main candidates for clinical PDT. In contrast, complexation of Pc with open shell, paramagnetic ions, such as Cu^{2+} , Co^{2+} , or Ni^{2+} , affords MPc with low intersystem crossing effect and short triplet lifetimes, resulting in weak or even totally quenched PDT activities. Similar to the above-mentioned active PTT process, the latter complexes (CuPc , CoPc , and NiPc) are expected to display strong



heating effect under the excitation of an appropriate laser system. Herein, we chose three representative Pc compounds, PcC1, PcC2, and PcC3 (Fig. 4a), as a group of study objects to verify this expectation. The $^1\text{O}_2$ generation tests indicated that the photosensitizing ability of PcC1 was much lower than that of PcC2 (Table S1 †). In addition, the spectral studies showed

that PcC2 possesses strong fluorescence emission, while under the same condition, there is almost no fluorescent signal of PcC1 solution (Fig. S10 †). These results indicate that PcC1 is probably suitable for PTT, while PcC2 can be used for PDT.

As shown in Fig. S11, † under a laser irradiation (*e.g.* 685 nm, 1.0 W cm^{-2} , 10 min), $10\ \mu\text{M}$ of PcC1 in water with 0.1% CEL can induce a significant temperature increase with a ΔT of about $40\ ^\circ\text{C}$. In the same experimental settings, PcC2 does not trigger a different temperature variation from that of the control group. We also investigated the effect of PcC1 aggregation on its photothermal conversion using CEL as the pharmaceutical formulation. Compared with the visible aggregation of PcC1 in water with 0% or 0.1% CEL, PcC1 in water with 10% CEL was basically in the form of a monomer (Fig. S12a †). In addition, the non-aggregated PcC1 displayed a higher heating effect (Fig. S12b †) as compared to its aggregated form. Moreover, despite the fact that the structure of PcC3 also contains a paramagnetic metal, PcC3 shows a much lower heating effect as compared to that of PcC1 (Fig. 4b), which is probably a consequence of the much weaker absorption of PcC3 caused by its substantial aggregation in water with 10% CEL (Fig. 4c). These results demonstrate that both the paramagnetic Cu and the monomer formation contribute to PcC1's photothermal conversion.

To investigate the possibility of PcC1 for cancer cell inhibition, we carried out the cell cytotoxicity experiments with and without laser treatment. As shown in Fig. 4d, no significant cytotoxicity is observed for both PcC1 and PcC2 under dark conditions. However, in the presence of laser treatment, the inhibition of PcC1 ($5\ \mu\text{M}$) against HepG2 cell is $92.1 \pm 0.5\%$. In the same experimental settings, PcC2 only kills $52.5 \pm 1.9\%$ cells. Since its cellular temperature is much higher than $42\ ^\circ\text{C}$ (Fig. 4e) during treatment, we speculate that temperature increase, but not ROS generation (Fig. 4f), should be the main reason for the cell killing effect of PcC1, which is very different from the PDT effect of PcC2. In particular, to further prove this speculation, we also used an ice-bath to control the cells' temperature lower than $30\ ^\circ\text{C}$ during laser irradiation. As shown in Fig. S13, † the cell inhibition of PcC1 almost disappeared after avoiding their temperature increase, while PcC2 still shows an efficient photocytotoxicity.

These results clearly indicate that PcC1 is a good PTT agent for cancer cell inhibition because of its relaxation process through fluorescence emission and intersystem crossing (no ROS generation) is inhibited efficiently. Furthermore, it is not hard to broadly expand the purview of Pcs utility in PTT due to their diversified metal chelation.

The above studies indicate that the PTT effects of Pc compounds with a high Φ_F (>0.13) and Φ_Δ (>0.49) are not significant. To confirm its universality, we further studied the photothermal conversion of two zinc Pcs substituted with sulfonic acid groups PcD1 ($\Phi_F = 0.15$, $\Phi_\Delta = 0.72$) and PcD2 ($\Phi_F = 0.14$, $\Phi_\Delta = 0.82$). Their chemical structures and photophysical and photochemical properties are shown in Fig. 5 and Table S1. † The photothermal studies indicate that both of PcD1 and PcD2 have negligible heating effect (Fig. S14 †). These results indicate that the preliminary prediction of Pcs' PTT effect is

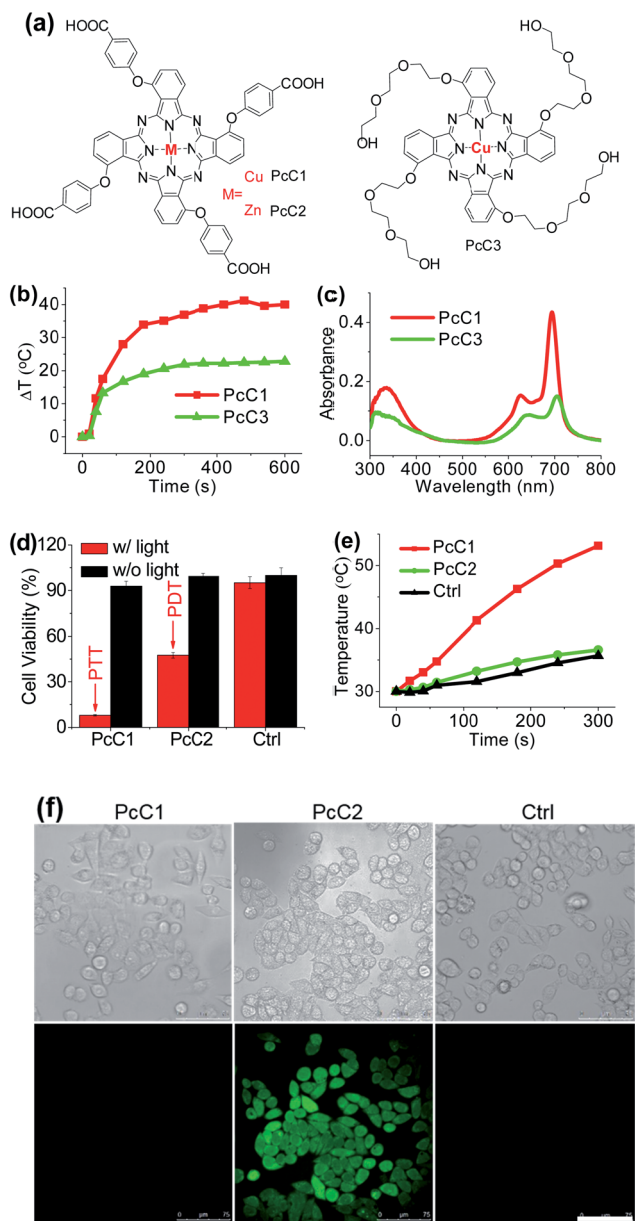


Fig. 4 (a) Chemical structures of PcC1, PcC2, and PcC3. Only the major C_{4h} isomers were shown for tetra-substituted Pcs, which likely present the other isomers. (b) Temperature variation profile of PcC1 and PcC3 (both at $10\ \mu\text{M}$) in water with 10% CEL after being exposed to 685 nm laser irradiation (1.0 W cm^{-2}). (c) Electronic absorption of PcC1 and PcC3 (both at $4\ \mu\text{M}$) in water with 10% CEL. (d) Cytotoxic effect of PcC1 and PcC2 (both at $5\ \mu\text{M}$) on HepG2 cells with and without laser irradiation (630 nm , 1.0 W cm^{-2} , 5 min). (e) Temperature profile of HepG2 cells induced by PcC1 and PcC2 under laser irradiation. Non-treated cells with laser irradiation were used as the control. (f) ROS levels in HepG2 cells transfected with PcC1 and PcC2 under laser irradiation. Scale bars = $75\ \mu\text{m}$.



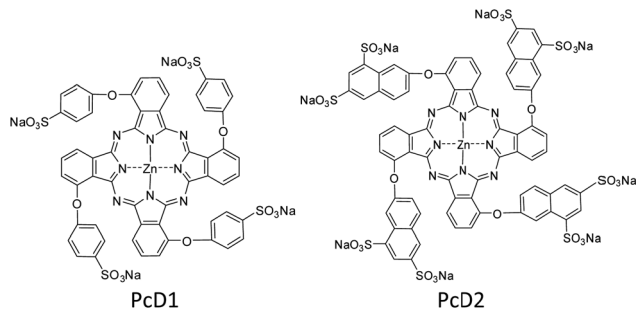


Fig. 5 Chemical structures of PcD1 and PcD2. Only the major C_{4h} isomers were shown for tetra-substituted Pcs, which likely present the other isomers.

available based on their photophysical and photochemical properties.

4. Comparison with the common molecular dye-based PTT agents

ICG and MB are two clinically approved molecular dyes that have been widely used as biophotonic contrast agents for phototheranostic applications.^{6c,16} To further highlight the unique photothermal properties of the above-mentioned Pcs, we thus compared their heating effects with those of ICG and MB under the same conditions. We can observe from Fig. 6 that only PcA1, PcB1, and PcC1 showed significant temperature elevation after 685 nm-laser irradiation. In addition, the values of their temperature variations are all about three times higher than those of both ICG and MB. Interestingly, despite their different absorption spectra (Fig. S15[†]), the optimal laser wavelengths of these molecular dyes (except ICG) for induction of best PTT effect are all at around 685 nm. This was found after comparing their PTT effects using laser systems at different wavelengths (630, 685, and 730 nm), but with the same power density (Fig. S16[†]). Even under 808 nm-laser irradiation (Fig. S17[†]), the PTT effect of ICG is still significantly lower than those of PcA1, PcB1, and PcC1. In addition, the decline in temperature variations of ICG and MB after 3 min-irradiation indicates their easy photobleaching. In contrast, PcA1 (Fig. 1d), PcB1 (Fig. S8a[†]), and PcC1 (Fig. S11a[†]) show much stronger photostability. Therefore, we believe that these specific Pcs, particularly the available but undeveloped Pcs

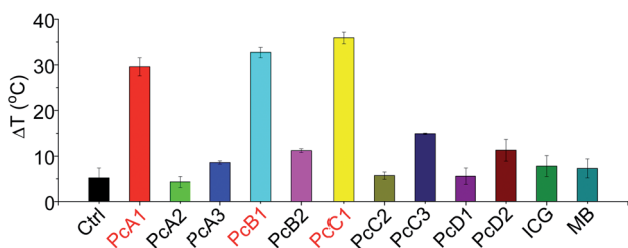


Fig. 6 Temperature variation of different molecular dyes (all at 10 μM) in water with 0.1% CEL after being exposed to laser irradiation (685 nm, 1.0 W cm^{-2}) for 10 min. Ctrl is only water with 0.1% CEL.

with more rational structure modifications, should enable molecular dye-based biophotonic contrast agents to play a better role in phototheranostics.

5. *In vivo* PTT efficiency

Encouraged by the unique PTT effect of PcA1, PcB1, and PcC1 *in vitro*, we tried to investigate their potential use as an *in vivo* PTT agent. Since only PcC1 showed total PTT effect and no PDT effect, we thus carried out preliminary mouse experiments using PcC1 to evaluate the *in vivo* PTT efficacy of Pcs on S180 tumors. For mice treated with PcC1 by intratumoral injection, the mean temperature at tumor sites increased to about 53 °C under 685 nm-laser irradiation for 10 min at a low power density of 0.2 W cm^{-2} (Fig. 7a and b). In comparison, the mean temperature of tumors treated with only laser irradiation increased to about 36 °C, indicating that PcC1 is efficient for *in vivo* photothermal conversion. In addition, the tumor growth of mice treated with both PcC1 and laser irradiation are significantly inhibited, while the mice treated with only PcC1 show similar tumor growth with control group (Fig. 7c). Moreover, the body weights of mice were not affected by these treatments (Fig. S18[†]), suggesting that the PTT treatment by PcC1 is biocompatible. Despite these encouraging results, we believe that higher *in vivo* PTT efficacy could be obtained using more rationally designed Pc molecular dyes, particularly with the structures bearing tumor-targeting groups.

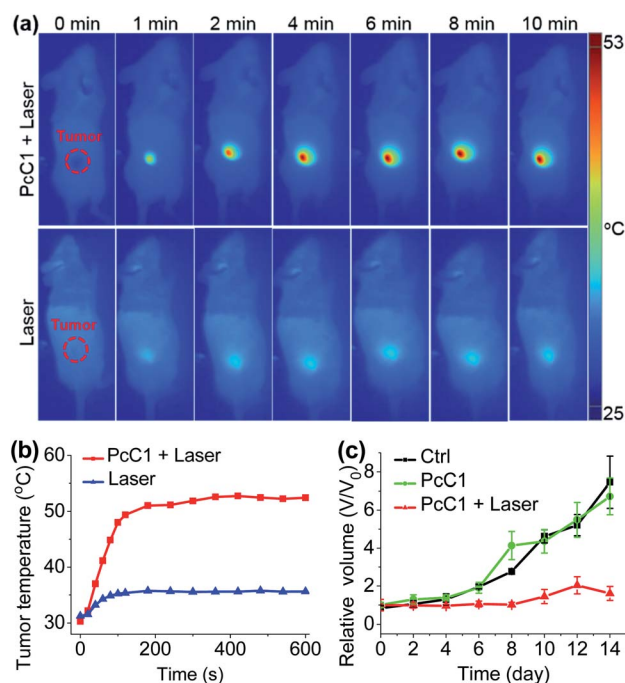


Fig. 7 *In vivo* PTT effect. (a) Thermal images of mice bearing S180 tumors treated with PcC1 (200 μM , 50 μL) under continuous laser irradiation (685 nm, 0.2 W cm^{-2}) for 10 min. (b) Temperature profile of tumor sites after treatments. (c) Tumor growth curves of the three groups of mice after treatments.



Conclusions

In conclusion, for the first time, we systematically demonstrated that Pc molecular dyes are also suitable for PTT except routine PDT. *In vitro* and *in vivo* evaluations demonstrate that the desired photothermal conversion induced by Pc compounds can be achieved through diversified structural modifications, including change in peripheral substituents, altering axial ligands, and changing central metal ions. By only considering their chemistry, Pcs exhibit this flexibility, providing the possibility for further screening and investigations, which rises hope for cancer phototherapy. The results should attract great interest of researchers related to PTT. Moreover, this study can thus stimulate and provide the ground for further development of Pc molecular dye-based multifunctional phototheranostic agents.

In vivo studies

Female mice (~20 g) were purchased from Vital River Co., Ltd, China. All animal studies were performed in compliance with guidelines of the Animal Care Committee of Fuzhou University. Meanwhile, all animal experiments were approved by the local Ethics Committee of Fuzhou University.

Conflicts of interest

There are no conflicts to declare.

Acknowledgements

This work is supported by National Natural Science Foundation of China (grants U1705282, 21473033, 21301031, 21172037).

Notes and references

- (a) R. Bonnett, *Chem. Soc. Rev.*, 1995, **24**, 19–33; (b) L. B. Josefsen and R. W. Boyle, *Theranostics*, 2012, **2**, 916–966; (c) Y. Zhang and J. F. Lovell, *Wiley Interdiscip. Rev.: Nanomed. Nanobiotechnol.*, 2017, **9**, e1420.
- (a) N. Sekkat, H. van den Bergh, T. Nyokong and N. Lange, *Molecules*, 2012, **17**, 98–144; (b) Z. Jiang, J. Shao, T. Yang, J. Wang and L. Jia, *J. Pharm. Biomed. Anal.*, 2014, **87**, 98–104; (c) X. Li, B. D. Zheng, X. H. Peng, S. Z. Li, J. W. Ying, Y. Zhao, J. D. Huang and J. Yoon, *Coord. Chem. Rev.*, 2017, DOI: 10.1016/j.ccr.2017.08.003.
- (a) D. E. J. G. J. Dolmans, D. Fukumura and R. K. Jain, *Nat. Rev. Cancer*, 2003, **3**, 380–387; (b) A. P. Castano, P. Mroz and M. R. Hamblin, *Nat. Rev. Cancer*, 2006, **6**, 535–545; (c) S. Pervaiz and M. Olivo, *Clin. Exp. Pharmacol. Physiol.*, 2006, **33**, 551–556; (d) J. F. Lovell, T. W. B. Liu, J. Chen and G. Zheng, *Chem. Rev.*, 2010, **110**, 2839–2857.
- (a) Z. Huang, *Technol. Cancer Res. Treat.*, 2005, **4**, 283–293; (b) Y. Zhang, L. He, J. Wu, K. Wang, J. Wang, W. Dai, A. Yuan, J. Wu and Y. Hu, *Biomaterials*, 2016, **107**, 23–32; (c) Y. Wang, Y. Lin, H. G. Zhang and J. Zhu, *J. Cancer Res. Clin. Oncol.*, 2016, **142**, 813–821; (d) X. Li, B. Y. Zheng, M. R. Ke, Y. Zhang, J. D. Huang and J. Yoon, *Theranostics*, 2017, **7**, 2746–2756.
- (a) Z. Zhou, J. Song, L. Nie and X. Chen, *Chem. Soc. Rev.*, 2016, **45**, 6597–6626; (b) I. S. Turan, D. Yildiz, A. Turksoy, G. Gunaydin and E. U. Akkaya, *Angew. Chem., Int. Ed.*, 2016, **55**, 2875–2878; (c) J. Kim, H. R. Cho, H. Jeon, D. Kim, C. Song, N. Lee, S. H. Choi and T. Hyeon, *J. Am. Chem. Soc.*, 2017, **139**, 10992–10995; (d) H. S. Jung, J. Han, H. Shi, S. Koo, H. Singh, H. J. Kim, J. L. Sessler, J. Y. Lee, J. H. Kim and J. S. Kim, *J. Am. Chem. Soc.*, 2017, **139**, 7595–7602; (e) S. Kolemen, T. Ozdemir, D. Lee, G. M. Kim, T. Karatas, J. Yoon and E. U. Akkaya, *Angew. Chem., Int. Ed.*, 2016, **55**, 3603–3610; (f) X. Li, S. Yu, D. Lee, G. Kim, B. Lee, Y. Cho, B. Y. Zheng, M. R. Ke, J. D. Huang, K. T. Nam, X. Chen and J. Yoon, *ACS Nano*, 2017, DOI: 10.1021/acsnano.7b07809.
- (a) Z. Zha, X. Yue and Z. Dai, *Adv. Mater.*, 2013, **25**, 777–782; (b) P. Liang, Q. Tang, Y. Cai, G. Liu, W. Si, J. Shao, W. Huang, Q. Zhang and X. Dong, *Chem. Sci.*, 2017, **8**, 7457–7463; (c) J. F. Lovell, C. S. Jin, E. Huynh, H. Jin, C. Kim, J. L. Rubinstein, W. C. Chan, W. Cao, L. V. Wang and G. Zheng, *Nat. Mater.*, 2011, **10**, 324–332; (d) Q. Zou, M. Abbas, L. Zhao, S. Li, G. Shen and X. Yan, *J. Am. Chem. Soc.*, 2017, **139**, 1921–1927; (e) L. Cheng, C. Wang, L. Z. Feng, K. Yang and Z. Liu, *Chem. Rev.*, 2014, **114**, 10869–10939; (f) X. Liang, Y. Li, X. Li, L. Jing, Z. Deng, X. Yue, C. Li and Z. Dai, *Adv. Funct. Mater.*, 2015, **25**, 1451–1462.
- (a) C. S. Jin, J. F. Lovell, J. Chen and G. Zheng, *ACS Nano*, 2013, **7**, 2541–2550; (b) H. S. Jung, J. H. Lee, K. Kim, S. Koo, P. Verwilst, J. L. Sessler, C. Kang and J. S. Kim, *J. Am. Chem. Soc.*, 2017, **139**, 9972–9978.
- (a) X. Li, C. Y. Kim, S. Lee, D. Lee, H. M. Chung, G. Kim, S. H. Heo, C. Kim, K. S. Hong and J. Yoon, *J. Am. Chem. Soc.*, 2017, **139**, 10880–10886; (b) L. Du, H. Qin, T. Ma, T. Zhang and D. Xing, *ACS Nano*, 2017, **11**, 8930–8943; (c) C. K. Lim, J. Shin, Y. D. Lee, J. Kim, K. S. Oh, S. H. Yuk, S. Y. Jeong, I. C. Kwon and S. Kim, *Theranostics*, 2012, **2**, 871–879.
- K. K. Ng and G. Zheng, *Chem. Rev.*, 2015, **115**, 11012–11042.
- (a) X. J. Jiang, J. D. Huang, Y. J. Zhu, F. X. Tang, D. K. P. Ng and J. C. Sun, *Bioorg. Med. Chem. Lett.*, 2006, **16**, 2450–2453; (b) X. J. Jiang, P. C. Lo, S. L. Yeung, W. P. Fong and D. K. Ng, *Chem. Commun.*, 2010, **46**, 3188–3190; (c) X. J. Jiang, P. C. Lo, Y. M. Tsang, S. L. Yeung, W. P. Fong and D. K. Ng, *Chem.–Eur. J.*, 2010, **16**, 4777–4783; (d) E. van de Winkel, R. J. Schneider, A. de la Escosura and T. Torres, *Chem.–Eur. J.*, 2015, **21**, 18551–18556; (e) R. C. H. Wong, P. C. Lo and D. K. P. Ng, *Coord. Chem. Rev.*, 2017, DOI: 10.1016/j.ccr.2017.10.006; (f) X. H. Peng, S. F. Chen, B. Y. Zheng, B. D. Zheng, Q. F. Zheng, X. S. Li, M. R. Ke and J. D. Huang, *Tetrahedron*, 2017, **73**, 378–384.
- (a) Z. Jiang, J. Shao, T. Yang, J. Wang and L. Jia, *J. Pharm. Biomed. Anal.*, 2014, **87**, 98–104; (b) M. R. Ke, D. K. P. Ng and P. C. Lo, *Chem. Commun.*, 2012, **48**, 9065–9067; (c) J. T. F. Lau, P. C. Lo, X. J. Jiang, Q. Wang and D. K. P. Ng, *J. Med. Chem.*, 2014, **57**, 4088–4097; (d) W. L. Lan, F. R. Liu, M. R. Ke, P. C. Lo, W. P. Fong, D. K. P. Ng and



- J. D. Huang, *Dyes Pigm.*, 2016, **128**, 215–225; (e) Q. Sun, B. Y. Zheng, Y. H. Zhang, J. J. Zhuang, M. R. Ke and J. D. Huang, *Dyes Pigm.*, 2017, **141**, 521–529.
- 12 D. Jaque, L. Martínez Maestro, B. Del Rosal, P. Haro-Gonzalez, A. Benayas, J. L. Plaza, E. Martín Rodríguez and J. García Solí, *Nanoscale*, 2014, **6**, 9494–9530.
- 13 S. Wang, L. Shang, L. Li, Y. Yu, C. Chi, K. Wang, J. Zhang, R. Shi, H. Shen, G. I. N. Waterhouse, S. Liu, J. Tian, T. Zhang and H. Liu, *Adv. Mater.*, 2016, **28**, 8379–8387.
- 14 (a) H. Lu and N. Kobayashi, *Chem. Rev.*, 2016, **116**, 6184–6261; (b) T. Nyokong, *Pure Appl. Chem.*, 2011, **83**, 1763–1779; (c) Y. Zhou, D. Wang, Y. Zhang, U. Chitgupi, J. Geng, Y. Wang, Y. Zhang, T. R. Cook, J. Xia and J. F. Lovell, *Theranostics*, 2016, **6**, 688–697.
- 15 H. Ali and J. E. van Lier, *Chem. Rev.*, 1999, **99**, 2379–2450.
- 16 (a) A. L. Vahrmeijer, M. Hutteman, J. R. van der Vorst, C. J. van de Velde and J. V. Frangioni, *Nat. Rev. Clin. Oncol.*, 2013, **10**, 507–518; (b) Q. Chen, L. Xu, C. Liang, C. Wang, R. Peng and Z. Liu, *Nat. Commun.*, 2016, **7**, 13193; (c) H. Moon, J. Kang, C. Sim, J. Kim, H. Lee, J. H. Chang and H. Kim, *J. Controlled Release*, 2015, **218**, 63–71; (d) P. Huang, P. Rong, A. Jin, X. Yan, M. G. Zhang, J. Lin, H. Hu, Z. Wang, X. Yue, W. Li, G. Niu, W. Zeng, W. Wang, K. Zhou and X. Chen, *Adv. Mater.*, 2014, **26**, 6401–6408; (e) J. Zhang, Z. Liu, P. Lian, J. Qian, X. Li, L. Wang, W. Fu, L. Chen, X. Wei and C. Li, *Chem. Sci.*, 2016, **7**, 5995–6005.

